



First validation of high-resolution satellite-derived methane emissions from an active gas leak in the UK

Emily Dowd^{1,2}, Alistair J. Manning³, Bryn Orth-Lashley⁴, Marianne Girard⁴, James France^{5,6}, Rebecca E. Fisher⁵, Dave Lowry⁵, Mathias Lanoisellé⁵, Joseph R Pitt⁷, Kieran M. Stanley⁷, Simon O'Doherty⁷,
5 Dickon Young⁷, Glen Thistlethwaite⁸, Martyn P. Chipperfield^{1,2}, Emanuel Gloor⁹, Chris Wilson^{1,2}

¹School of Earth and Environment, University of Leeds, Leeds, UK

²National Centre for Earth Observation, University of Leeds, Leeds, UK

³Hadley Centre, Met Office, Exeter, UK

10 ⁴GHGSat Inc., Montreal, Canada

⁵Department of Earth Sciences, Royal Holloway, University of London, Egham, UK

⁶Environmental Defense Fund, 41 Eastcheap, London, UK

⁷School of Chemistry, University of Bristol, Bristol, UK

⁸UK National Atmospheric Emissions Inventory, Ricardo Energy & Environment, Harwell, Oxon, UK

15 ⁹School of Geography, University of Leeds, Leeds, UK

Correspondence to: Emily Dowd (eed@leeds.ac.uk)

Abstract. Atmospheric methane (CH₄) is the second most important anthropogenic greenhouse gas and has a 20-year global warming potential 82 times greater than carbon dioxide (CO₂). Anthropogenic sources account for ~60% of global CH₄ emissions, of which 20% come from oil & gas exploration, production and distribution. High-resolution satellite-based imaging spectrometers are becoming important tools for detecting and monitoring CH₄ point source emissions, aiding mitigation. However, validation of these satellite measurements, such as those from the commercial GHGSat satellite constellation, has so far not been documented for active leaks. Here we present the monitoring and quantification, by GHGSat's satellites, of the CH₄ emissions from an active gas leak from a downstream natural gas distribution pipeline near Cheltenham, UK in
20 Spring/Summer 2023, and provide the first validation of the satellite-derived emission estimates using surface-based mobile greenhouse gas surveys. We also use a Lagrangian transport model, NAME, to estimate the flux from both satellite and ground-based observation methods and assess the leak's contribution to observed concentrations at a local tall tower site (30 km away). We find GHGSat's emission estimates to be in broad agreement with those made from the in-situ measurements. During the study period (March-June 2023) GHGSat's emission estimates are 236 - 1357 kg CH₄ hr⁻¹ whereas the mobile surface
30 measurements are 886 - 998 kg CH₄ hr⁻¹. The large variation is likely down to variations in flow through the pipe and engineering works across the 11-week period. Modelled flux estimates in NAME are 181-1243 kg CH₄ hr⁻¹, which are lower than the satellite- and mobile survey-derived fluxes but are within the uncertainty. After detecting the leak in March 2023, the local utility company was contacted, and the leak was fixed by mid-June 2023. Our results demonstrate that GHGSat's observations can produce flux estimates that broadly agree with surface-based mobile measurements. Validating the accuracy
35 of the information provided by targeted, high-resolution satellite monitoring shows how it can play an important role in identifying emission sources, including for unplanned fugitive releases that are inherently challenging to identify, track and



estimate their impact and duration. Rapid access to such evidence to inform local action to address fugitive emission sources across the oil and gas supply chain could play a significant role in reducing the anthropogenic contribution to climate change.

1 Introduction

40 The increase in atmospheric methane (CH_4) has contributed an extra 23% to the radiative forcing in the troposphere since 1750 and has a 20-year global warming potential 82 times greater than carbon dioxide (CO_2) (Forster et al., 2021; Saunio et al., 2020). CH_4 has a mixture of natural and anthropogenic sources. Anthropogenic sources account for ~60% of global CH_4 emissions, of which 20% come from oil & gas exploitation and transportation (Saunio et al., 2020). The United Kingdom (UK) contributes 0.48% (European Commission, 2022) to global anthropogenic CH_4 emissions and 9% of UK emissions are
45 from fugitive emissions from fuels (National Atmospheric Emissions Inventory (NAEI) Pollutant Information, Methane, 2023). Fugitive emissions of CH_4 from oil and gas distribution in the UK were estimated to be 187.3 kilotonnes of CH_4 in 2020 (NAEI Pollutant Information, Methane, 2023). Natural gas is mostly composed of CH_4 (Bains et al., 2016) and fugitive emissions are unintentional releases of substances, such as natural gas, making them difficult to estimate. In the UK, fugitive emissions of natural gas from low-pressure distribution, medium pressure gas mains and above-ground installations are
50 currently estimated by individual utility companies using an industry wide Shrinkage and Leakage model (SLM). The model combines parameters including: pipeline length, an annual leakage rate and an average system pressure correction to estimate fugitive emissions, which are then aggregated to give a UK estimate (Marshall, 2023). The leakage rates are determined by sampling pipes during National Leakage Tests commissioned by the UK Gas Distribution Networks (GDN, Gas Governance, 2020). However, regular monitoring of pipes and detection of leaks through other methods such as emission identification and
55 source rate quantification from high-resolution satellite observations and in-situ monitoring could be incorporated into leakage estimates to improve frequency of quantification and validate estimates.

At the 27th United Nations Convention on Climate Change Conference of Parties (COP27), the United Nations Environment Programme (UNEP) International Methane Emissions Observatory (IMEO) announced its Methane Alert and Response
60 System (MARS) (United Nations Environment Programmes, 2023). MARS uses TROPOMI on board Sentinel-5P to identify very large methane plumes ($> 25,000 \text{ kg h}^{-1}$, Lauvaux et al., 2022) and other very large methane hot spots, and combines other satellite instruments such as ASI PRISMA to attribute the plume to a specific source. The IMEO then informs relevant governments and organisations of the large methane emissions. MARS is an example of how high-resolution satellite-based imaging spectrometers, such as TROPOMI and ASI PRISMA, are becoming important tools for detecting and monitoring CH_4
65 point source emissions, aiding mitigation. TROPOMI has a pixel size of $5.5 \text{ km} \times 7 \text{ km}$ with a detection threshold of $25,000 \text{ kg h}^{-1}$ (Lauvaux et al., 2022) and ASI PRISMA $30 \text{ m} \times 30 \text{ m}$ with a detection threshold of $500\text{-}2,000 \text{ kg h}^{-1}$ (Guanter et al., 2021). GHGSat was the first satellite constellation launched specifically for CH_4 point-source emission identification, quantification, and attribution, and was the first system to provide high-resolution data to IMEO, although these data are not



incorporated into MARS. GHGSat's constellation provides global monitoring of sites that are potentially emitting above 100
70 kg h⁻¹ and also targets locations based on detected emissions using Sentinel-5P or Sentinel-2 (Schuit et al., 2023). Not all leaks
can be detected by global monitoring satellites, such as Sentinel-5P or Sentinel-2, due to their high detection threshold and
lower resolution and so GHGSat's ability to detect smaller sources is important for observing leaks that might otherwise go
undetected and unreported. However, there is a trade-off between global monitoring satellites and GHGSat because GHGSat
requires a target to observe. GHGSat has previously detected CH₄ emissions from a variety of sources including landfill sites,
75 coal mining and natural gas pipelines (GHGSat, 2022; ESA, 2023; GHGSat, 2023). Validation of GHGSat's technology has
been performed on controlled releases and blind validation tests (McKeever and Jervis, 2022; Sherwin et al., 2023). However,
validation of the emission estimates from the satellite constellation has so far not been documented for active leaks. Here we
present the detection, monitoring and quantification, by GHGSat's satellites, of CH₄ emissions from an active gas leak near
Cheltenham, UK in Spring/Summer 2023, and provide the first study using surface-based mobile greenhouse gas surveys to
80 validate GHGSat's estimates. We provide estimates of the leak by three different methods: i) GHGSat-derived fluxes using
the Integrated Mass Enhancement Method (IME); ii) Fluxes derived from ground-based observations using a Gaussian Plume
model; and iii) Estimates from plumes simulated by the UK Met Office's Numerical Atmospheric-dispersion Modelling
Environment (NAME, Jones et al., 2007) and scaled to match the satellite and mobile survey observations. We also estimate
mole fractions from the leak at a local tall tower monitoring site using NAME. We compare the modelled mole fractions from
85 the gas leak with the observed above-background concentrations and discuss the implications of the leak in terms of the UK
National Atmospheric Emissions Inventory (NAEI) and the success in monitoring and mitigating it.

2 Methods

2.1 Gas Leak Location

As part of a research study, the University of Leeds requested, through the Third Party Missions Programme with the European
90 Space Agency (ESA), that GHGSat monitor a landfill site near the town of Cheltenham, UK. By chance the monitored area
included the location of a large (> 100 kg h⁻¹) gas leak (within 1 km of the landfill) allowing it to be detected by the satellite
constellation. The landfill site was found to be below the detection threshold. The gas leak was first detected by GHGSat
during its first cloud-free overpass on 27th March 2023 and the location of the leak from the satellite was estimated to be
51.95088°N, 2.09962°W at approximately 33 m above sea level (m.a.s.l). When GHGSat detect an emission from a site which
95 is not in their database, other datasets such as visible satellite imagery and infrastructure maps are used to determine the source.
In this case, GHGSat confirmed the source by contacting the utility company. The leak was from a low-pressure gas distribution
pipeline situated in a field next to a railway line, approximately 5 km north of Cheltenham. The UK gas pipeline network is
currently being upgraded from old metal pipes to new plastic ones and it is likely that the gas leak came from an older pipe
(Wales & West Utilities, 2023). The GHGSat satellite constellation monitored the site over approximately 11 weeks (6
100 successful observations) until the leaking pipe was repaired. The area surrounding the leak is a mixture of pastoral and arable



agricultural land with one farm ~70 m to the east of the site, two waste management sites less than half a kilometre to the south and a small residential area less than 200 m to the east and southeast of the leak location. The farm closest to the site rears cattle so they are also a likely source of CH₄ to the atmosphere along with manure produced by other animals, although these sources are much more diffuse. There is one single carriageway road to the south of the leak location, which passes within ~30
105 m of the estimated location of the gas leak. The leak location estimated here is an approximate location for the surface emission and is not necessarily the precise location of the pipeline break.

2.2 Atmospheric Methane Measurements

2.2.1 GHGSat Satellite Measurements

GHGSat is a constellation of 9 SmallSats (~15 kg) orbiting in low Earth orbit at altitudes ranging from 500 – 550 km which
110 retrieve vertical column density of CH₄ and detect concentration enhancements above background from targeted industrial facilities globally. The satellite retrievals are collected using a Wide-Angle Fabry-Perot (WAF-P) imaging spectrometer, which is a hyperspectral spectrometer operating in the short-wave infrared (SWIR) at 1630 – 1675 nm, where methane absorption lines can be resolved for each pixel in the 12 km × 12 km sensor field-of-view (Jervis et al., 2021). This sensor system achieves
115 both high spatial and spectral resolution, enabling precise geolocation and low noise measurements. For the 8 commercially operating satellites (GHGSAT-C1 to C8), the system achieves a spatial resolution of 25 m and spectral resolution of 0.3 nm (Jacob et al., 2022), having the capability of a 1-2 day revisit time. This allows for precise attribution of CH₄ emission enhancements to sources with emission rates above 100 kg h⁻¹ (50% probability of detection at wind speeds of 3 m/s). The performance of the system has been independently verified through controlled releases of CH₄ at known rates that were measured using the GHGSat system (Sherwin et al., 2023).

120 The raw images collected by the satellites are processed through GHGSat's proprietary toolchain. The surface reflectance and column-averaged concentration of CH₄ in parts per billion (ppb) are retrieved for each pixel by fitting a model of the instrument and atmosphere. These data are georeferenced using satellite's GPS outputs and Landsat-8 imagery with sub-pixel accuracy, achieving a geolocation accuracy of ~25 m for the source location.

2.2.2 Mobile Greenhouse Gas Observations

125 Royal Holloway, University of London's (RHUL) mobile greenhouse gas laboratory was used for ground-based verification of the leak location, source type and emission rate. The mobile laboratory includes a suite of cavity enhanced laser absorption spectrometers for the measurement of CH₄, CO₂ and ethane (C₂H₆) mole fractions and methane isotopes (δ¹³C-CH₄): Picarro G2311-f (10 Hz CH₄ and CO₂), Licor-7810 (1 Hz CH₄ and CO₂), LGR UMEA - ultraportable methane ethane analyser (1 Hz CH₄ and C₂H₆) and Picarro G2210-i (1 Hz CH₄, CO₂, C₂H₆ and δ¹³C-CH₄). The instruments are powered using a 6 kW portable
130 lithium power station (Goal Zero Yeti 6000). Air is pumped to the instruments from inlets on the roof of a hybrid car, 1.8 m above ground level. A sonic anemometer (Campbell CSAT3B 3-D) and GPS receiver are also installed on the roof of the



vehicle. Another air inlet is connected to a diaphragm pump for filling 3 litre multilayer foil bags with air, for subsequent high precision methane $\delta^{13}\text{C}$ analysis by isotope ratio mass spectrometry (Fisher et al., 2006) and methane mole fraction analysis using the Licor-7810. The air bags were filled when the car was parked in and outside of the emissions plume. Instruments are
135 harmonised to international scales for CH_4 and CO_2 at RHUL using cylinders of ambient air calibrated by NOAA (National Oceanic and Atmospheric Administration).

Mobile surveys were carried out during daytime on 26th May, 12th June and 22nd June 2023. These dates were chosen because the wind direction was from between NW and ENE, allowing the emissions plume to be measured on the nearest road which was to the south of where GHGSat had identified the source. During each survey the car was driven at 20-30 mph (32-48 km/h)
140 downwind of the emissions site with at least 12 passes.

2.3 Flux Estimation Methods

2.3.1 GHGSat Flux Estimation

The satellite-derived fluxes are estimated using the Integrated Mass Enhancement (IME) method (Varon et al., 2018). First, the emission signal is identified and masked by isolating methane enhancements that are not instrument artefacts or signal
145 from albedo features. The source location is determined based on wind direction derived from Goddard Earth Observing System Forward Processing (GEOS-FP, NASA GMAO, 2023), the methane enhancement gradient and morphology caused by the emission. The IME method relates the emission source rate to the emission mass downwind of the source (defined by the masked methane concentration and the source location) based on the expected transport of methane in the wind (defined by the GEOS-FP wind data). The uncertainty on the source rate includes the uncertainties on the wind speed, the methane
150 enhancement and the IME model parameters.

2.3.2 Gaussian Plume Inversion Method

The flux estimates from the mobile greenhouse gas measurements were calculated using a Gaussian plume model to determine the mole fraction of a gas as a function of distance downwind of a point source (Seinfeld and Pandis, 2006). We use this model, developed by Pasquill and Smith (1983), to estimate the emission rate of the source using the concentrations observed
155 downwind of the plume to scale an idealised Gaussian plume model. In the idealised model, the mole fraction at a point in the plume is a function of flux of the source (Q , kg h^{-1}), advective horizontal wind speed (u , ms^{-1}), the rate of dispersion and the distance from the source, see Eq. 1. The plume measured during each transect during the mobile survey was manually identified in the dataset and distance and angle to the emission source calculated. We used a mean of the source locations provided by the satellite retrievals as the source location in the model. We then used the observed concentration data and wind speed data
160 (26th May data utilised the vehicle 10Hz sonic anemometer data, whereas the 12th June used data from the Met Office's UKV model due to instrument availability) to create the initial model plume using Eq. 1.

$$C(x, y, z) = \frac{Q}{\pi\sigma_y\sigma_z u} \exp\left(-\frac{y^2}{2\sigma_y^2}\right) \left[\exp\left(-\frac{(z-h)^2}{2\sigma_z^2}\right) + \exp\left(-\frac{(z+h)^2}{2\sigma_z^2}\right) \right] \quad (1)$$



Where C is the atmospheric concentration of methane at (x, y, z) , x is the distance downwind from the source (m), y is the distance crosswind (m), z is the height above ground level (m), Q is the source strength (kg h^{-1}), σ_y and σ_z are the diffusion coefficients in the crosswind and vertical directions respectively, u represents the horizontal time-averaged wind speed (ms^{-1}) and h is the height of the release (m). The dispersion coefficients of the plume (σ_y and σ_z) are approximated using Brigg's assumptions in the Pasquill-Gifford atmospheric stability classification.

To scale from the idealised plume to the measurements, the flux through a control surface of 1m height and the width of the plume is determined using the measurement data (Eq. 2)

$$\sum (c_i[\text{CH}_4] \cdot \Delta x_i \cdot \Delta z) \quad (2)$$

where c_i is the concentration of point i , Δx_i is the distance driven by the car at this point, and $\Delta z=1$ m is the vertical extent of the control surface. The corresponding control surface flux is then calculated for the modelled plume and the ratio between measured control surface flux and modelled control surface flux used to scale the model to the measured plume.

There are several assumptions made when using the Gaussian plume model. We assume that the source is emitting at a constant rate, the CH_4 mass is conserved and there are no additional sources or sinks during transport. We also assume that the wind speed and vertical eddy diffusivity are constant, the diffusion in the x direction and horizontal wind shear is negligible and the molecular diffusion is negligible compared to turbulent diffusion. Local baseline CH_4 is taken as the 2nd percentile measurement over a 5-minute moving average window as per other mobile campaign. However, only measurements more than 1 ppm above baseline concentrations were used in the calculation of gas leak flux to conservatively ensure that the total is not enhanced by any small emissions from surrounding sources such as the farm or waste sites. The baseline was calculated using the methods described in Fernandez et al. (2022). The uncertainty ranges provided are due to the variability in each plume transect and do not reflect the added uncertainty from the limitations of the Pasquill stability classifications or from the imperfect knowledge of the exact leak location.

2.4 NAME Dispersion Modelling

We simulated the dispersion of the gas leak through a suite of experiments using the UK Met Office's Numerical Atmospheric-dispersion Modelling Environment (NAME, Jones et al., 2007). We use NAME to estimate the flux of the leak using the observed concentrations from both GHGSat and the mobile survey to provide some continuity between the two observation and flux estimation techniques. We also modelled the leak's mole fractions of CH_4 at Ridge Hill (RGL) tall tower site (30 km away) and compared them to the observed above-background concentrations at RGL.

NAME is a Lagrangian dispersion model which simulates the transport and dispersion of chemical species through the atmosphere (Jones et al., 2007). The model is offline and for this study is driven by the Met Office's Numerical Weather Prediction (NWP) meteorology from the high-resolution UKV model. The UKV meteorology has a horizontal resolution of $1.5 \text{ km} \times 1.5 \text{ km}$ and 70 vertical levels over the UK with hourly temporal resolution. NAME follows individual theoretical particles during the simulation and the number of particles within the user-defined grid determines the total mass output per grid cell for each time step. Model particles are advected by three-dimensional wind fields provided by the NWP model and



are dispersed using random walk techniques which account for turbulent velocity structures in the atmosphere (Jones et al., 2007). NAME includes additional parametrizations for atmospheric processes which are unresolved in the NWP, but which influence the transport of pollutants, including deep convection, horizontal mesoscale motions, and turbulence (Meneguz and Thomson, 2014; Webster et al., 2018). The output resolution of NAME is user-defined, allowing a suite of experiments to be performed at various resolutions. In our simulations we assume the chemical sinks of CH₄ to be negligible due to the short transport time to both the road near the leak site (~minutes, depending on wind direction) and to RGL (~7-10 hours, depending on wind direction) compared to the long atmospheric lifetime of CH₄ (~9 years, Prather et al., 2012).

In the first experiment, we set up a high-resolution grid in NAME to estimate the magnitude of the flux from the concentrations observed by the satellite and mobile survey. To estimate the flux using the satellite retrievals we simulated the gas leak with a unit release (1 gs⁻¹), starting 1 hour before the time of observation and simulated the release for three hours. The simulation was output with a horizontal resolution of 25 m × 25 m with a 500 m vertical resolution up to 1000 m a.g.l. and a 1-hourly time step. We selected the model time step closest to the observation time to do our analysis. We produced a pressure-weighted mean total column value from the two layers, where concentrations in the layer above 500 m were approximately 0 ppb. The modelled and observed plumes did not overlap well so we defined certain criteria in the modelled plume to capture the modelled dispersion of CH₄ in a way that is comparable with the GHGSat plume. We defined the plume by removing concentrations less than 1% of the maximum value and limited the length of the modelled plume to match the observed length of GHGSat's plume. This method assumes that the CH₄ emitted in NAME has travelled at the same distance and speed as detected by GHGSat. We integrated the CH₄ over the total column concentrations in both the GHGSat plume and the defined area of the NAME plume to obtain a scaling factor for the NAME flux. We then used this scaling factor to estimate the flux of the gas leak using NAME. To test the robustness of our modelled flux estimate we also calculated fluxes using two other plume definitions: (1) We removed values less than 1% of the maximum value; and (2) less 5% of the maximum value, ignoring the plume length criteria in both cases. We then scaled the model using the integrated mass from these defined plumes to test the robustness of the flux estimation method.

We applied a similar mass integration method to estimate the flux in NAME using the observations from the mobile survey. We simulated the gas leak with a unit release (1 gs⁻¹), starting 1 hour before the peak observation time and simulated the release for three hours. The model was output at a horizontal resolution of 10 m × 10 m with a single 2 m layer to capture the volume observed by the mobile survey. We selected three values centred on the maximum concentration in the model and mobile survey concentrations along the road that the survey was completed. In the model the selected values include the maximum value of the plume along the road and the two grid boxes either side of the maximum value. From the observations we used the median concentrations calculated from the different observed transects during the mobile survey, then selected maximum value and the observation taken before and after the maximum value. These values are approximately 10 m apart. We integrated across the three peak values for the model and mobile survey in order to scale the model and derived a modelled flux. We then calculated flux estimation uncertainties by taking the three grid boxes to the left and three grid boxes to the right of the peak value on the road and use the mass of these grid boxes to scale the model to the observed peak concentrations.



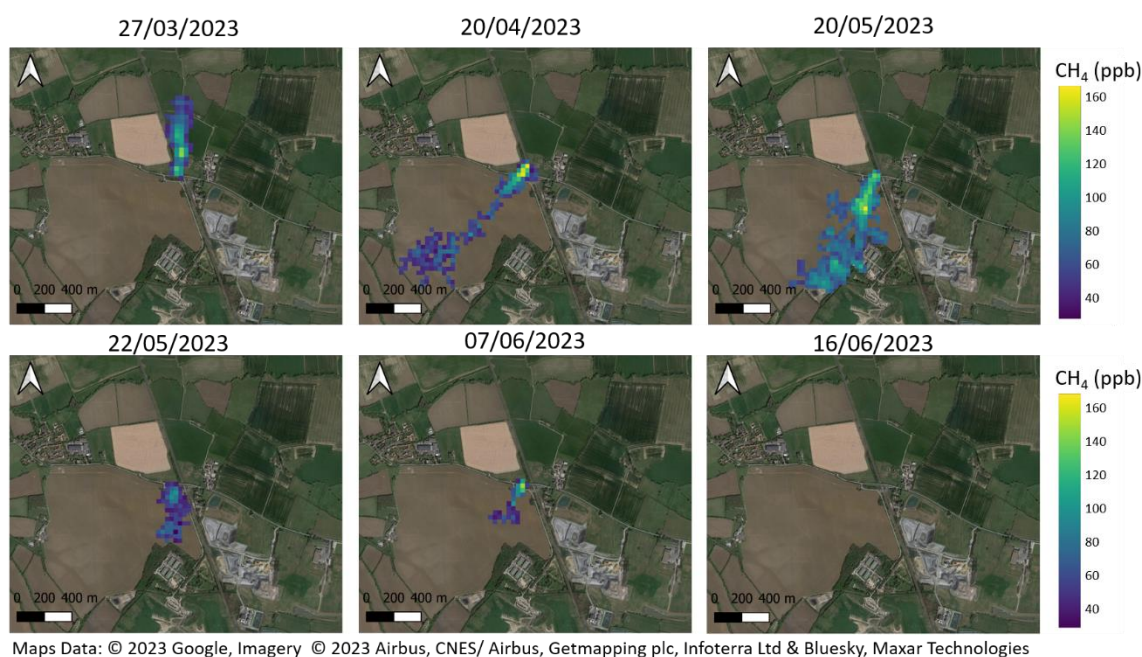
230 The second experiment involved estimating the leak's contribution to the observed above-background concentrations at the
nearby tall tower (RGL) and assessing the likelihood of the leak contributing to most of the observed above-background
concentration. We ran NAME with an output resolution of 2.5 km × 2.5 km with 40 m vertical resolution up to 120 m a.g.l. to
capture the height of the observations at RGL. We used the five observed emission rates provided by GHGSat. We simulated
the leak as a point source in NAME at 51.95088°N, 2.09962°W from 27th March to 13th June, with the emission rate being held
235 constant at each derived emission rate from the date that the observation was made until the date of the next available
observation (see Fig 3a). We also simulated the upper and lower uncertainty emission rate from the satellite-derived fluxes
(see Fig 3a). The model produced a one-hourly time series output at the RGL tall tower location at 80-120 m a.g.l. which we
compared to the above-background observations. This simulation is called 'NAME_spring'. Note, the prevailing wind at the
leak site is from the west/southwest but a north easterly wind is needed for the emissions from the leak to be transported to
240 RGL.

In the third experiment, we simulated the leak with the same model set up as NAME_spring but with two alternative constant
flux rates and simulated an extra year before the date that the leak was discovered, giving a simulation time of approximately
1 year and 5 months (1st March 2022 to 13th June 2023). We simulated both the maximum flux derived by GHGSat and the
maximum flux derived from the mobile survey separately. This simulation is called 'NAME_long'. We selected this time
245 period to cover a full year previous to the leak discovery, to assess the frequency of large contributions at RGL from a
theoretical leak over a longer time period, including different seasons. It should be noted that the UK DECC network was set
up to monitor long-term greenhouse gas concentrations across the UK and is not specifically designed to detect fugitive
emissions, like this gas leak. However, due to the location of the tall tower site relative to the gas leak in this case (within 30
km), it is reasonable to consider whether it might have been possible to use statistical analysis and inverse modelling techniques
250 to recognise that the leak was ongoing without the use of GHGSat.



3 Results

3.1 Observations and Flux Comparisons



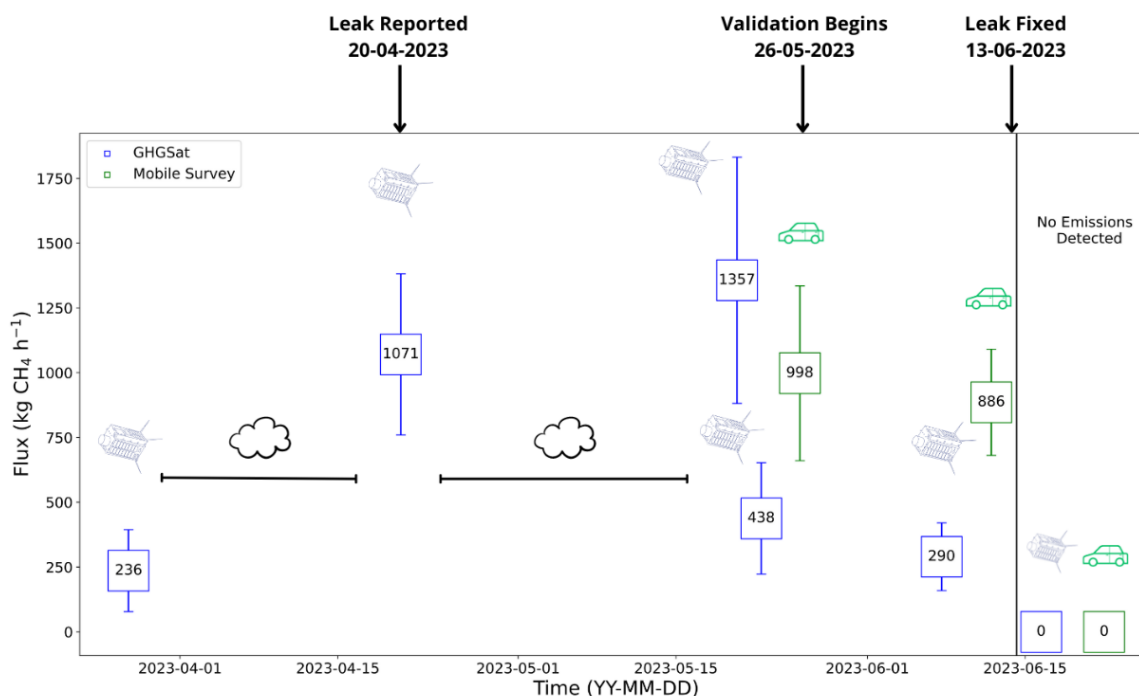
255 **Figure 1. Total column CH₄ (ppb) observations from the GHGSat satellite showing the variation in strength and size of the plume from the gas leak on six dates between March and June 2023.**

We first observed an enhancement over a field, which was later confirmed to be a gas leak, on 27th March 2023 via satellite when targeting a nearby landfill site. After detecting the leak, GHGSat continued to monitor the site to quantify how much CH₄ was being released. Figure 1 shows the methane plumes measured by the satellite between 27th March and 16th June 2023. The initial observation on 27th March produced a flux estimate from the leak of $236 \pm 157 \text{ kg h}^{-1}$ and the peak observed leak rate occurred on 20th May with an estimated flux rate of $1375 \pm 481 \text{ kg h}^{-1}$. The observations taken after 20th May show that the size and strength of the plume was decreasing, with the last observed emission on 7th June with an estimated flux rate of $290 \pm 130 \text{ kg h}^{-1}$. The satellite-derived fluxes were estimated using the IME method. The next successful observation on 16th June shows no emissions above the 100 kg h^{-1} detection threshold.

265 During the satellite observation period, we conducted mobile greenhouse gas surveys of the leak to validate the satellite measurements. On 26th May and 12th June, observed CH₄ mole fractions were large enough to be above the dynamic range (20 ppm but capable up to 60 ppm) of the Picarro G2311-f when driving through the plume. The LI-7810 data were therefore used for the Gaussian plume modelling. The maximum CH₄ mole fractions recorded in each pass were 77 - 588 ppm (77,000 - 588,000 ppb) on 26th May and 120 - 839 ppm (120,000 - 839,000 ppb) on 12th June. Gaussian plume estimates of the flux were estimated to be $998 \pm 377 \text{ kg h}^{-1}$ on 26th May and $886 \pm 205 \text{ kg h}^{-1}$ on 12th June. The ethane/methane ratio in the plume was



270 0.05 and the $\delta^{13}\text{C}$ isotopic signature was -36.7 ± 2.1 ‰. These values are characteristic of the thermogenic gas in the UK gas network (Zazzeri et al., 2015; Lowry et al., 2020), and confirm that the leak was from a gas pipeline. On 22nd June there were no significant enhanced concentrations recorded downwind of the leak site.



275 **Figure 2. Timeline of events during the observation period of the gas leak and the flux estimates (kg CH₄ h⁻¹) from the different instruments. The satellite-derived fluxes are in blue and the mobile survey-derived fluxes are in green.**

Figure 2 shows the timeline of events, including estimated fluxes (with their uncertainty), from both estimation methods. Also shown are the dates that the leak was reported to the utility company, when work started on the leak, when the leak was resolved according to the utility company and when there were no further emissions detected by satellite or mobile survey. Once the persistence of the leak was confirmed on 20th April, GHGSat contacted the utility company. Then work started on assessing and repairing the leak by the utility company on 27th April. GHGSat continued to monitor the leak and validation of the satellite retrievals by mobile survey began on 22nd May. We directly compare the flux estimates derived from the satellite and mobile surveys. Cloud obstructed the view of the satellite on the mobile survey days, so we compare the mobile survey-derived fluxes with the most recent satellite-derived flux to validate the satellite fluxes. We compare the mobile survey-derived flux on 26th May (998 ± 377 kg h⁻¹) and 12th June (886 ± 205 kg h⁻¹) with the satellite-derived flux on 22nd May (438 ± 215 kg h⁻¹) and 7th June (290 ± 131 kg h⁻¹), respectively, finding that the mobile survey-derived fluxes are higher than the satellite derived fluxes on these dates. However, both sets of fluxes have relatively large uncertainties, predominantly due to wind speed estimates used in the flux estimation, and the uncertainties overlap for the fluxes derived from the two observation



methods on 22nd and 26th May, see Fig. 1. The uncertainties for the fluxes in June do not overlap and this could be due to various factors such as variation in the flow of gas through the pipe or disruption due to the utility company working on the pipe. The mobile survey-derived fluxes compare well with the satellite fluxes derived in April and May. Differences between the satellite and ground survey fluxes will be discussed in detail in Sect. 4.

3.2 Flux Estimations from NAME Plume Modelling

We also use NAME to obtain a modelled estimate of the gas leak on each observation date for GHGSat and mobile survey observations to allow continuity between different observation and flux estimation methods. We simulated the gas leak with a unit release (1 gs^{-1}) and then used the observed concentrations to scale NAME to estimate the flux as discussed in Sect. 2.4. Table 1 shows the flux estimations from GHGSat and the mobile survey and their corresponding flux estimation, with the bounds of the estimation quoted in brackets from NAME. The NAME-derived flux estimations are smaller than the GHGSat-derived fluxes, but are always within the GHGSat uncertainty (Table 1). The smallest flux observed by GHGSat on 27th March was estimated to be $236 \pm 157 \text{ kg h}^{-1}$ and we estimate a flux of 181 [133, 322] kg h^{-1} , with a difference of 23% (55 kg h^{-1}) compared with the central estimate of the GHGSat-derived flux. The bounds of the NAME-derived flux estimations described in Sect. 2.4 are shown in brackets. The largest flux observed by GHGSat on 20th May was estimated to be $1375 \pm 481 \text{ kg h}^{-1}$ and we estimate a flux of 1243 [931, 2322] kg h^{-1} , with a difference of 10% (132 kg h^{-1}) compared with the central estimate of the GHGSat-derived flux. The estimation uncertainties for the NAME-derived fluxes are much larger than the GHGSat-derived fluxes on 20th April and 20th May and this is likely due to higher wind speeds used in the model compared with the wind speeds used in GHGSat's IME method (see Supplement, Table S2).

We also simulated the gas leak in NAME to derive a flux from the mobile survey observations. The NAME-derived fluxes are lower than the mobile survey-derived fluxes but they lie within the mobile survey estimation uncertainty (Table 1). The peak concentrations measured during the mobile survey were larger on 12th June than the concentrations measured on 26th May. However, the Gaussian plume model estimates a large flux on 26th May due to differences in wind speeds on the observation days. The NAME-derived flux is larger on 12th June than the NAME-derived flux on 26th May. The NAME-derived fluxes use the same wind speeds as the Gaussian plume model so differences between the model and the mobile survey fluxes are likely due to differences in the peak location along the road and the model resolution.

315

320

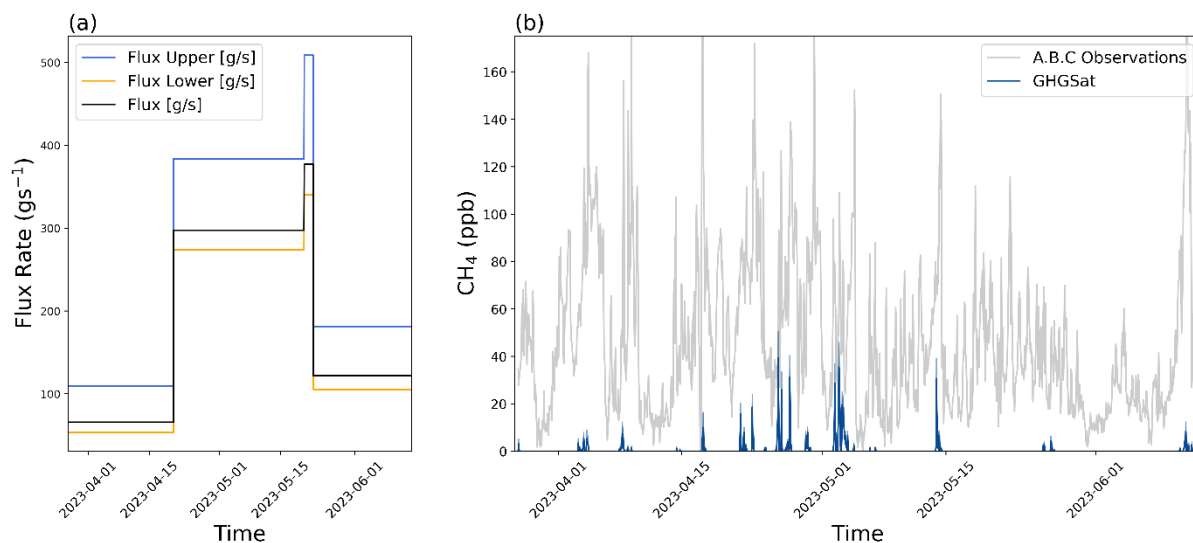


Table 1. The comparison between the mobile survey and GHGSat-derived fluxes (kg h^{-1}) and the equivalent fluxes derived in NAME (kg h^{-1}). The bounds of NAME-derived fluxes are shown in brackets.

Date	Mobile Survey Flux (kg h^{-1})	NAME-Derived Flux from MS Concentrations (kg h^{-1})	GHGSat Flux (kg h^{-1})	NAME-Derived Flux from GHGSat Concentrations (kg h^{-1})
27/03/2023	-	-	236 ± 157	181 [133, 322]
20/04/2023	-	-	1071 ± 310	745 [539, 1376]
20/05/2023	-	-	1375 ± 481	1243 [931, 2322]
22/05/2023	-	-	438 ± 215	384 [173, 292]
26/05/2023	998 ± 377	406 [366, 680]	-	-
07/06/2023	-	-	290 ± 131	204 [77, 244]
12/06/2023	886 ± 205	512 [498, 681]	-	-

3.3 Modelled Concentrations at Tall Tower Site

We carried out two simulations in NAME to assess the likelihood of the leak contributing to most of the observed above-background concentrations at RGL, described in Section 2.4. The occasions when the gas leak concentrations contribute to most of the above-background concentrations at RGL are defined as simulated concentrations that are at least two standard deviations (2σ , 14 ppb) larger than the observed background concentrations and contributing a significant percentage ($\geq 90\%$) of the above-background concentrations - we call this a ‘pollution event’. We investigated the number of pollution events at RGL over the period of the leak to assess whether statistical analysis and inverse modelling techniques can be used to recognise the gas leak. Figure 3b shows that the observed above-background concentrations at RGL are almost always much larger than the contributions from the gas leak during the NAME_spring simulation. We calculated the number of times the gas leak concentration was at least 2σ larger than the background concentration at RGL, i.e. when the leak’s contribution was above the noise of the background concentrations, and when it contributed to a ‘leak pollution event’ ($> 2\sigma$ and $> 90\%$ above-background) at RGL. Table 2 shows the results of these criteria during the NAME_spring simulation with hourly output. In the NAME_spring simulation, concentrations were above 2σ of the background concentrations 21 times and a ‘leak pollution event’ only occurred once. The enhancements due to the gas leak were larger than the noise of the background for at least one hour on 8 of the 79 simulated days. The single pollution event from the NAME_spring simulation shows that although CH_4 from the gas leak can make up a large portion of the above-background concentrations at RGL, this does not happen frequently and therefore it is not sufficient for statistical analysis or inverse modelling to identify the leak due to the significant contributions from other local sources.



345

Figure 3. (a) Varying flux rates (gs⁻¹) used in the NAME model simulation ‘NAME-spring’. (b) Modelled mole fractions (ppb) at the Ridge Hill (RGL) tall tower site from GHGSat-derived flux rates in the NAME-spring simulation (blue) and observed above-background mole fractions at RGL (grey).

350 The results from the NAME_spring simulation show that the frequency of ‘leak pollution events’ at RGL was low, therefore we investigated the gas leak contribution at RGL over a longer period (NAME_long). The NAME_long simulation is a hypothetical situation in which the gas leak is emitting at its highest estimated rate (from both observation methods) for much longer than we actually observed the leak. Similar to the NAME_spring, the above-background concentrations at RGL during the NAME_long simulation period were much larger than the concentrations modelled from the gas leak at RGL, making it

355 difficult to determine pollution events (see Supplement, Fig. S5). We applied the same criteria as the NAME_spring and found that during the NAME_long simulation the leak concentrations at RGL were 2σ above the background concentrations 226 times when using the GHGSat flux, and 140 times when using the mobile survey flux. The gas leak was above the noise of the background concentrations for at least one hour on 80 of 470 simulated days when using the satellite-derived flux. When we simulate the gas leak using the mobile survey-derived flux we find the gas leak to be above the noise of background

360 concentrations on 63 days for at least one hour. The gas leak also meets the ‘leak pollution event’ criteria 18 times for the GHGSat flux and 13 times for the mobile survey flux. ‘Leak pollution events’ from the gas leak occurred on 12 of 470 simulation days for at least one hour when simulating the satellite-derived flux and on 7 days when simulating the mobile survey-derived flux. The majority of the ‘leak pollution events’ occurred during April 2023. Based on these figures, the frequency of ‘leak pollution events’ from the gas leak during the NAME_long simulation is very low even when we assume

365 that the gas leak is constantly emitted at the highest estimated flux rates. This means that it is difficult to recognise the gas leak above the noise of the background concentrations and to determine the flux of the gas leak using inverse modelling techniques and observations at RGL. Both the NAME_spring and NAME_long simulations show there is a low number of ‘leak pollution



events' from the gas leak at RGL, which makes it difficult to recognise whether the above-background concentrations are from the leak or from other local sources.

370

Table 2. Number of one-hour periods simulated concentrations at Ridge Hill from the gas leak were at least 2σ larger than the background concentrations (B.C.) and number of times a pollution event occurs ($> 2\sigma$ B.C. and $> 90\%$ of the above background concentrations (A.B.C.)). The columns denoted with “upper” and “lower” represent the upper and lower uncertainty flux from the satellite and mobile survey (MS) derived fluxes.

Criteria	NAME Simulation	GHGSat Lower	GHGSat Central	GHGSat Upper	MS Lower	MS Central	MS Upper
Flux (kg h^{-1})	NAME_spring	Variable	Variable	Variable	-	-	-
# of times $> 2\sigma$ B.C.	NAME_spring	20	21	25	-	-	-
# of times $> 2\sigma$ B.C. and $> 90\%$ of A.B.C.	NAME_spring	1	1	2	-	-	-
Flux (kg h^{-1})	NAME_long	893	1367	1841	621	998	1375
# of times $> 2\sigma$ B.C.	NAME_long	115	226	285	47	140	229
# of times $> 2\sigma$ B.C. and $> 90\%$ of A.B.C.	NAME_long	10	18	39	3	13	19

375 **4 Discussion**

In this study we detected, monitored and validated fluxes of a large gas leak from a low-pressure gas distribution pipe near Cheltenham, UK. The global monitoring satellite Sentinel-5P was not able to detect this leak during its overpass times because it was obstructed by clouds and the emission rate was lower than its theoretical detection threshold ($25,000 \text{ kg h}^{-1}$, Lauvaux et al., 2022). The GHGSat satellite constellation has demonstrated it can detect down to 42 kg h^{-1} (McKeever and Jervis, 2022) and up to $79,000 \text{ kg h}^{-1}$ (GHGSat, 2022). As a result, the Cheltenham gas leak is well within the detection threshold of GHGSat. The GHGSat retrievals are predominantly during a north (N) or north easterly (NE) wind which means that the enhancement detected by the satellite will mostly be from the leak due to few CH_4 sources upwind of the leak. The N/NE wind is useful for comparisons with the mobile survey and our tall tower model simulations because RGL is situated to the west of the gas leak. However, the first satellite retrieval on 27th March is during southerly wind. No emissions from the landfill were detected by GHGSat which implies that emissions from the landfill are below 100 kg h^{-1} , possibly lower than 42 kg h^{-1} . Also, by the time the landfill emissions reach the gas leak location the CH_4 concentrations would be more diffuse resulting in very small percentage of the mole fraction in the retrieved pixel of the plume so the effect of the landfill upwind of the gas leak on this day is considered negligible.

385



We also confirmed and assessed the leak by completing a mobile survey on 26th May and 22nd June. The measured
390 concentrations on 22nd June were higher and the associated flux was lower than the equivalent concentrations and fluxes on
26th May, likely due to higher estimated wind speeds on 26th May. The Gaussian plume model has large uncertainties due to a
number of factors: e.g. the variability in the measured plume from changes in wind speed and direction, the lack of granularity
in the Pasquill classification (Fredenslund et al., 2019) and the lack of certainty over the exact position of the leak itself.

The satellite-derived flux estimates and flux estimates based on the ground-based measurements display some differences.
395 These could be due to actual differences in the leak rate on different days from changes in pipeline pressure or biases between
the two measurement and flux estimation methods. There are significant uncertainties associated with both flux estimation
methods which overlap for the satellite and mobile survey estimates on 22nd and 26th May, respectively. The second mobile
survey resulted in similar fluxes to the first survey and both were much larger than those estimated by GHGSat during the
same week. Unfortunately, we were unable to obtain satellite retrievals on the same days as the mobile measurements due to
400 obstruction by clouds. Since we were monitoring a live leak, it is likely that changes in flow through the pipe and engineering
works will have caused variations in the flux, contributing to the differences between the satellite and mobile survey estimates.
During the second mobile survey, on 12th June, repairs on the pipe were being carried out, so it is likely that emissions included
more diffuse emissions from a wider area of excavated soil (see Supplement, Fig. S1). In addition to the effects of actual leak
rate variations at the site, the satellite and mobile survey used different methods to estimate the fluxes, based on different
405 meteorology. However, despite the mobile measurement fluxes being measured on different days, they agree well with the
April and May satellite estimations. Based on the available observations, it is difficult to be certain whether the leak rate did
drop in late May, as suggested by the GHGSat data, or continued at high rates as suggested by the mobile survey.

The mobile survey allowed us to validate the gas leak by confirming the CH₄ detected by the satellite was present and through
isotope measurements also confirmed the source was natural gas. There are differences in the satellite-derived fluxes the mobile
410 survey-derived fluxes but even though we were monitoring a live leak, they are still of the same magnitude.

In order to provide some continuity between the different observation and flux estimation types we estimated the flux of the
gas leak in NAME using the observed concentrations from the satellite retrievals and the mobile survey. We find that the
NAME fluxes follow the same temporal flux pattern but are slightly lower than the GHGSat flux estimations. The difference
between the GHGSat-derived fluxes and the NAME-derived fluxes could be due to a number of reasons. The satellite plume
415 did not overlap well with the modelled plumes, making it difficult to define a plume shape that captured the dispersion of the
modelled plume well. We used a 25 m × 25 m horizontal resolution with 1.5 km resolution meteorology in NAME, which
means the model might not capture local wind effects on the plume, leading to differences in the plume direction. The model
simulations were run using a unit release making it difficult to define the plume shape using the threshold value GHGSat
applies to their retrievals (Jervis et al., 2021) or apply any concentration thresholds based on the GHGSat retrievals because
420 the modelled concentrations are not yet representative of the gas leak. Therefore, we applied three different criteria, described
in Section 2.4, to the modelled plume to get flux estimations. The NAME-derived fluxes using the GHGSat concentrations are
dependent on the plume selection criteria (see Table 1), particularly for larger fluxes, during 20th April and 20th May, where



the bounds of the estimation are much larger. This could be due to different wind speeds used in the model and the IME method used by GHGSat when deriving the fluxes; the wind speed in NAME is generally higher than GEOS-FP (see Supplement. 425 Table S2) and wind speeds are the largest uncertainty in the GHGSat IME flux estimation method (Jervis et al., 2021).

We also applied a similar method to estimate the fluxes in NAME using the observations from the mobile survey. We also find that the peak mixing ratios of the simulated plume does not align well with the peak mixing ratios from the mobile survey. This is likely due to the model meteorology not capturing local wind effects in this area. The road where the survey was conducted was approximately 30 m away from the estimated source location at its closest point, but at this point the car is 430 either ascending or descending the railway bridge which is not accounted for in the model. We find that NAME-derived flux using the mobile survey observations is smaller than the Gaussian plume model estimates, despite using the same wind speeds. Differences between flux estimates could be due to different parameterisations in the NAME model compared with the Gaussian plume, for example the Gaussian plume model assumes a neutral boundary layer and uses different dispersion assumptions. We are also sampling a very small section of the plume in the model, which might not fully represent the main 435 peak of the plume but was chosen to be similar in distance between the estimated source location and mobile survey observations. Also, during the mobile survey, instantaneously-measured concentrations from the gas leak fluctuated significantly whilst driving through the plume, showing predominately perturbations in atmospheric mixing. These effects are averaged out slightly when the emission is calculated because it incorporates multiple transects over a 30-minute period, some of these perturbations will still remain and the NAME model averages them out in the 1 hourly model time step.

The NAME-derived fluxes do provide some continuity between the different flux estimation methods because they show a 440 similar temporal pattern. The NAME-derived fluxes still peak on 20th April and fluctuate in a similar pattern to the other estimation methods in May and June. This implies that there were fluctuations in the leaking gas, likely due to repairs on the pipe were being carried out in May and June. Also the variation between the NAME-derived fluxes from both observation methods is smaller than the differences between the satellite derived fluxes using the IME method and the mobile-survey 445 derived fluxes using the Gaussian Plume method. This implies that the flux estimation methodologies are responsible for some differences between the satellite and mobile survey-derived fluxes.

Another uncertainty in modelling the flux in NAME from both the satellite and the mobile survey observations is the location of the leak. Four out of five locations were clustered together and these were used to calculate the mean location for the NAME modelling and for the Gaussian plume modelling. One estimated location was positioned on the other side of the road to the 450 actual leak and was considered as an outlier. We perturbed the leak location in the model by 10 m north (N), south (S), east (E) and west (W) to investigate the impact of the source location on the NAME flux estimates. Perturbing the source location shows that the mean location for the previous NAME simulations give the lowest flux values. We also find that the flux estimations are lower than the satellite-derived fluxes, apart from on 20th May (see Supplement, Table S1). The NAME fluxes, including the bounds of the estimation, derived on 20th May in the N/S/E/W directions are all higher than the satellite-derived 455 flux and the NAME-derived flux at the mean location. This shows that the flux estimation is also highly dependent on the



precise location of the leak when comparing with the GHGSat derived fluxes, particularly when the fluxes are large (e.g. 20th April and 20th May).

We also ran simulations in NAME to assess the frequency of the gas leak's contribution to the observed CH₄ at the nearby tall tower site, RGL. This method assumes that the meteorology and transport of CH₄ from the gas leak in the model is correct, however it is likely that local meteorological effects and the surrounding terrain (e.g. the nearby railway bridge) will have some influence on transport of CH₄ from the gas leak to RGL. We assessed the frequency of pollution events during our both NAME_spring and NAME_long simulations and found a low number of 'leak pollution events'. The results show that it is possible for the gas leak to contribute to a pollution at RGL. However, the low number of events means that it is difficult to estimate the location and magnitude of the flux using inverse modelling techniques. There are a number of different sources surrounding RGL which contribute to above-background concentrations such as agriculture, waste and fossil fuels from nearby towns and cities. When the wind is coming from the gas leak to RGL, the main sources near to the gas leak site are from pastoral and arable agriculture, household waste landfills and food waste recycling. The addition of these other methane sources being transported to RGL also adds further complexity to the above-background signal at RGL.

The coverage of the tall tower network in the UK is sparse and not specifically designed for monitoring time-limited fugitive emissions like this gas leak and these simulations show that it is unlikely that the RGL observations can be used to investigate a gas leak of this size, location and duration. In fact, in this case it was fortuitous that the gas leak was close to a tall tower site at all – due to the sparse coverage of the UK DECC network most gas leaks would likely not be near an observation site. Regular high-resolution satellite monitoring will allow us to detect emission locations, before monitoring them further through ground-based and drone-based surveys. However, GHGSat needs to be directed to observe the correct area in order to observe an emission. An 'early-warning' system to tell GHGSat would be useful in determining locations for the satellite to target. For example, Schuit et al., 2023 have developed a machine learning model to detect emission plumes in Sentinel-5P measurements and then GHGSat can be used to identify and quantify emissions at a higher resolution. However, in this case the gas leak would not have been detected by Sentinel-5P, so other methods should be developed to detect smaller emissions. A disadvantage of monitoring methane emissions via satellite in the UK is that the country is often covered in cloud. However, GHGSat has a frequent revisit time of 1-2 days and with more satellites coming online there is an increased chance of a successful observation. A hybrid monitoring system combining satellite retrievals and mobile surveys could enable the operational detection of fugitive emissions and enhance countries capabilities to reduce CH₄ emissions.

We investigated whether emission estimates from this gas leak would be reported in the UK's National Atmospheric Emissions Inventory (NAEI), which is funded by the UK Government's Department for Sustainability and Net Zero (DESNZ) and the Department for Environment, Food and Rural Affairs (Defra). The NAEI estimates emissions to the atmosphere from all anthropogenic sources, including CH₄, from gas leakage across the UK's National Transmission Network (operated by National Grid) and the downstream gas networks that are operated by Wales and West Utilities (WWU) and other GDN operators (such as Cadent, Northern Gas Networks, and SGN). The NAEI receives annual submissions from each of the GDNs to provide annual estimates of gas leakage from their distribution networks, using an industry-wide SLM. The SLM enables



490 GDNs to apply consistent methods to generate emission estimates from several different source types across the gas network,
with specific methods developed and agreed across the sector for: Above Ground Installations (leakage, venting), Low pressure
pipe leakage, medium pressure pipe leakage, own gas use, theft and Third Party Damage. The annual gas leakage estimates
are also reported by each of the GDNs to Ofgem as part of the network price control and performance mechanisms (Ofgem,
2023). For the gas leak detected by GHGSat, WWU would estimate the leakage of gas due as described in Marshall, 2023
495 which would be included in the annual estimate reported to NAEI. The annual submissions to the NAEI do not provide
incident-specific estimates because the annual leakage estimates are aggregated prior to reporting to the NAEI. Therefore, the
transparency and completeness of those reported emission estimates, including from Third Party damage incidents, such as
this gas leak, is uncertain.

In addition to detecting and monitoring the leak, GHGSat contacted the relevant utility company who took steps to fix the leak.
500 The utility company confirmed that the leak was fixed on 13th June. This is a good example of how satellite data can be used
to detect fugitive emissions and inform facility operators of their emissions, encouraging them to take action to fix leaks. We
estimate over 11 weeks with a mean emission rate of 754 kg h⁻¹, the gas would have leaked a total of 1,393,392 kg of CH₄.
Using the United States Environmental Protection Agency's Greenhouse Gas Equivalencies calculator (Greenhouse Gas
Equivalencies Calculator, 2023), we estimate the mass of CH₄ lost to be 39,015 tonnes of CO₂ equivalent, which is equivalent
505 to the emissions from the annual electricity consumption of 7,500 homes.

5 Conclusion

In this study, we detected and monitored a gas leak from a low-pressure distribution pipeline near Cheltenham, UK using
GHGSat's high-resolution satellite constellation. We also validated the leak by completing two ground based mobile
greenhouse gas surveys and found differences with the satellite-derived fluxes, likely due to observations taking place on
510 different days. During the observation period, the satellite-derived fluxes varied from 236-1357 kg h⁻¹ and the mobile
measurement derived fluxes were between 886-996 kg h⁻¹. The mobile survey measurements agree better with earlier satellite
estimates on 20th April and 20th May than the retrievals taken in late May and June covering the same weeks as the mobile
survey, although they were not made concurrently with the satellite observations. We also estimated the gas leak flux using
the NAME model to provide some continuity between the different flux estimation methods. We find that the fluxes in NAME
515 are smaller than both the satellite- and mobile survey-derived fluxes but are within the uncertainty of both and more consistent
with each other. We also assessed the gas leak's contribution at the nearby tall tower site, RGL. The UK DECC network is
sparse and was not specifically designed to detect fugitive emissions. Our simulations show that for a gas leak 30 km from
RGL we cannot provide a confident estimate of the flux rate using the RGL observations and inverse modelling techniques
and it was not likely that any significantly large above-background concentrations would have stood out in the observations.
520 Steps taken by GHGSat to inform the utility company also led to mitigation, which is a good example of how satellites can be
used to aid companies and government bodies in reducing their emissions. This study shows that GHGSat has the capability



to detect and monitor fugitive emissions over 100 kg h^{-1} within the UK. The UK has access to mobile measurement laboratories, which can aid in monitoring CH_4 whilst the views from satellites are obscured by cloud. This gas leak was coincidentally discovered whilst trying to measure emissions from a nearby landfill. The discovery of this very large fugitive emission (by
525 UK standards) raises the question of how many other large gas leaks are happening in the UK that are going undetected or unresolved. Although there are no current plans to carry this out operationally, combining satellite observations and mobile surveys means that the UK can access the technology to regularly monitor for fugitive emissions and take steps to significantly reduce their CH_4 emissions. It would seem prudent for the UK to explore how multiscale measurement methods currently used, primarily for academic research, can be moved into operational modes to assist with leak detection and repair programmes for
530 the GDN. Currently, the focus on methane intensity and emissions reduction is on the upstream sector, but events such as these suggest that significant challenges face the distribution networks too.

This study highlights the capability of GHGSat and ground-based mobile surveys in monitoring fugitive emissions. Despite some differences in the emission estimates likely due to issues inherent in monitoring an active and variable leak, it is an excellent case study in validating satellite technology and collaborating with industry to reduce the human impact on climate
535 change.

Code and Data Availability

The UK Met Office NAME model and UM output to drive NAME are available via a research licence from the UK Met Office. UK DECC network data from Ridge Hill covering this period have been submitted to the Centre for Environmental Data
540 Analysis archive (<https://catalogue.ceda.ac.uk/uuid/f5b38d1654d84b03ba79060746541e4f>). The mobile survey data and GHGSat plume rasters will become available once the paper has been published. The GHGSat code is proprietary information and will not be made publically available.

Author Contributions

ED, AJM, CW, EG and MPC designed the study. BO and MG processed and applied IME method for the GHGSat retrievals. JF, REF and DL carried out the ground-based surveys, ML analysed the isotope measurements and JF applied the Gaussian
545 Plume method. Tall tower data was collected by JRP, KMS, SO and DY. GT provided expertise on the national emissions inventory and reporting requirements. ED carried out analysis of emissions estimates and NAME simulations with guidance from AJM and CW. All co-authors contributed to the writing and analysis of the results.

Competing Interests

The authors declare they have no conflict of interest.



550 Acknowledgements

The GHGSat data provided for this project was through the European Space Agency Third Party Missions Programme. We would like to thank Alison Redington at the Met Office for her support in setting up daily forecasts to help identify suitable satellite tasking dates. We also like to thank Susan Leadbetter, Nicola Stebbing and Frances Beckett at the Met Office for their expertise in setting up high-resolution NAME simulations.

555 Financial Support

This work was supported by the Natural Environment Research Council (NERC) SENSE CDT studentship (NE/T00939X/1). This work was also supported by NERC grants NE/V006924/1 and NE/V011863/1. Royal Holloway's mobile laboratory (MIGGAS) was funded by a NERC capital grant (NE/T009268/1). The Royal Holloway greenhouse gas group is supported by NERC research grants on UK greenhouse gas and global methane studies (NE/S003657/1 and NE/V000780/1). The UK
560 DECC network is funded by the UK Government DESNZ under contracts TRN1028/06/2015, TRN1537/06/2018 and TRN5488/11/2021 to the University of Bristol and through the National Measurement System at the National Physical Laboratory. The collection of atmospheric composition data at Ridge Hill is also supported by the Integrated Carbon Observation System (ICOS). TRN 1537/06/2018 also provides support to AJM.

References

565 Bains, M., Hill, L., and Rossington, P.: Material comparators for end-of-waste decisions. Fuels: Natural Gas, Environment Agency, 2016.

Satellites detect large methane emissions from Madrid landfills:
https://www.esa.int/Applications/Observing_the_Earth/Satellites_detect_large_methane_emissions_from_Madrid_landfills,
last access: 31 August 2023.

570 European Commission: EDGAR (Emissions Database for Global Atmospheric Research) Community GHG Database (a collaboration between the European Commission, Joint Research Centre (JRC), the International Energy Agency (IEA), and comprising IEA-EDGAR CO₂, EDGAR CH₄, EDGAR N₂O, EDGAR F-GASES version 7.0, 2022.

Fernandez, J. M., Maazallahi, H., France, J. L., Menoud, M., Corbu, M., Ardelean, M., Calcan, A., Townsend-Small, A., van der Veen, C., Fisher, R. E., Lowry, D., Nisbet, E. G., and Röckmann, T.: Street-level methane emissions of Bucharest, Romania
575 and the dominance of urban wastewater., *Atmospheric Environment: X*, 13, 100153, <https://doi.org/10.1016/j.aeaoa.2022.100153>, 2022.

Fisher, R., Lowry, D., Wilkin, O., Sriskantharajah, S., and Nisbet, E. G.: High-precision, automated stable isotope analysis of atmospheric methane and carbon dioxide using continuous-flow isotope-ratio mass spectrometry, *Rapid Commun Mass Spectrom*, 20, 200–208, <https://doi.org/10.1002/rcm.2300>, 2006.



580 Forster, P., Storelvmo, K., Armour, W., and Collins, W. J.: 2021: The Earth's Energy Budget, Climate Feedbacks, and Climate Sensitivity. In *Climate Change 2021: The Physical Science Basis. Contribution of Working Group I to the Sixth Assessment Report of the Intergovernmental Panel on Climate Change*, n.d.

Fredenslund, A. M., Mønster, J., Kjeldsen, P., and Scheutz, C.: Development and implementation of a screening method to categorise the greenhouse gas mitigation potential of 91 landfills, *Waste Management*, 87, 915–923, 585 <https://doi.org/10.1016/j.wasman.2018.03.005>, 2019.

Gas Governance: Shrinkage and Leakage Model Review 2020, Joint Distribution Network Publication, 2020.

GHGSat: GHGSat measures its largest emission from a single source ever from Nord Stream 2 leak, 2022.

Coal Mining Methane Emissions | Case Study - GHGSat: <https://www.ghgsat.com/en/case-studies/coal-mining-methane/>, last access: 31 August 2023.

590 Guanter, L., Irakulis-Loitxate, I., Gorroño, J., Sánchez-García, E., Cusworth, D. H., Varon, D. J., Cogliati, S., and Colombo, R.: Mapping methane point emissions with the PRISMA spaceborne imaging spectrometer, *Remote Sensing of Environment*, 265, 112671, <https://doi.org/10.1016/j.rse.2021.112671>, 2021.

Jacob, D. J., Varon, D. J., Cusworth, D. H., Dennison, P. E., Frankenberg, C., Gautam, R., Guanter, L., Kelley, J., McKeever, J., Ott, L. E., Poulter, B., Qu, Z., Thorpe, A. K., Worden, J. R., and Duren, R. M.: Quantifying methane emissions from the 595 global scale down to point sources using satellite observations of atmospheric methane, *Atmospheric Chemistry and Physics Discussions*, 1–44, <https://doi.org/10.5194/acp-2022-246>, 2022.

Jervis, D., McKeever, J., Durak, B. O. A., Sloan, J. J., Gains, D., Varon, D. J., Ramier, A., Strupler, M., and Tarrant, E.: The GHGSat-D imaging spectrometer, *Atmospheric Measurement Techniques*, 14, 2127–2140, <https://doi.org/10.5194/amt-14-2127-2021>, 2021.

600 Jones, A., Thomson, D., Hort, M., and Devenish, B.: The U.K. Met Office's Next-Generation Atmospheric Dispersion Model, NAME III, Borrego C. and Norman A.-L. (Eds) *Air Pollution Modeling and its Application XVII, Proceedings of the 27th NATO/CCMS International Technical Meeting on Air Pollution Modelling and its Application.*, 580–589, 2007.

Lauvaux, T., Giron, C., Mazzolini, M., d'Aspremont, A., Duren, R., Cusworth, D., Shindell, D., and Ciais, P.: Global assessment of oil and gas methane ultra-emitters, *Science*, 375, 557–561, <https://doi.org/10.1126/science.abj4351>, 2022.

605 Lowry, D., Fisher, R. E., France, J. L., Coleman, M., Lanoisellé, M., Zazzeri, G., Nisbet, E. G., Shaw, J. T., Allen, G., Pitt, J., and Ward, R. S.: Environmental baseline monitoring for shale gas development in the UK: Identification and geochemical characterisation of local source emissions of methane to atmosphere, *Science of The Total Environment*, 708, 134600, <https://doi.org/10.1016/j.scitotenv.2019.134600>, 2020.

610 Marshall, M.: Gas Governance: Shrinkage and Leakage Model Review, Joint Distribution Network Publication, February 2023, 2023.

McKeever, J. and Jervis, D.: *Validation and Metrics for Emissions Detection by Satellite*, 2022.

Meneguz, E. and Thomson, D. J.: Towards a new scheme for parametrisation of deep convection in NAME III, *International Journal of Environment and Pollution*, 54, 128–136, <https://doi.org/10.1504/IJEP.2014.065113>, 2014.

615 NAEI Pollutant Information, Methane: https://naei.beis.gov.uk/overview/pollutants?pollutant_id=3, last access: 1 August 2023.



GMAO - Global Modelling and Assimilation Office Research Site:
https://gmao.gsfc.nasa.gov/GMAO_products/NRT_products.php, last access: 30 August 2023.

Network price controls 2021-2028 (RIIO-2): <https://www.ofgem.gov.uk/energy-policy-and-regulation/policy-and-regulatory-programmes/network-price-controls-2021-2028-riio-2>, last access: 19 September 2023.

620 Prather, M. J., Holmes, C. D., and Hsu, J.: Reactive greenhouse gas scenarios: Systematic exploration of uncertainties and the role of atmospheric chemistry, *Geophysical Research Letters*, 39, <https://doi.org/10.1029/2012GL051440>, 2012.

Saunio, M., Stavert, A. R., Poulter, B., Bousquet, P., Canadell, J. G., Jackson, R. B., Raymond, P. A., Dlugokencky, E. J., Houweling, S., Patra, P. K., Ciais, P., Arora, V. K., Bastviken, D., Bergamaschi, P., Blake, D. R., Brailsford, G., Bruhwiler, L., Carlson, K. M., Carrol, M., Castaldi, S., Chandra, N., Crevoisier, C., Crill, P. M., Covey, K., Curry, C. L., Etiope, G., Frankenberg, C., Gedney, N., Hegglin, M. I., Höglund-Isaksson, L., Hugelius, G., Ishizawa, M., Ito, A., Janssens-Maenhout, G., Jensen, K. M., Joos, F., Kleinen, T., Krummel, P. B., Langenfelds, R. L., Laruelle, G. G., Liu, L., Machida, T., Maksyutov, S., McDonald, K. C., McNorton, J., Miller, P. A., Melton, J. R., Morino, I., Müller, J., Murguía-Flores, F., Naik, V., Niwa, Y., Noce, S., O'Doherty, S., Parker, R. J., Peng, C., Peng, S., Peters, G. P., Prigent, C., Prinn, R., Ramonet, M., Regnier, P., Riley, W. J., Rosentreter, J. A., Segers, A., Simpson, I. J., Shi, H., Smith, S. J., Steele, L. P., Thornton, B. F., Tian, H., Tohjima, Y., Tubiello, F. N., Tsuruta, A., Viovy, N., Voulgarakis, A., Weber, T. S., van Weele, M., van der Werf, G. R., Weiss, R. F., Worthy, D., Wunch, D., Yin, Y., Yoshida, Y., Zhang, W., Zhang, Z., Zhao, Y., Zheng, B., Zhu, Q., Zhu, Q., and Zhuang, Q.: The Global Methane Budget 2000–2017, *Earth System Science Data*, 12, 1561–1623, <https://doi.org/10.5194/essd-12-1561-2020>, 2020.

635 Schuit, B. J., Maasackers, J. D., Bijl, P., Mahapatra, G., Van den Berg, A.-W., Pandey, S., Lorente, A., Borsdorff, T., Houweling, S., Varon, D. J., McKeever, J., Jervis, D., Girard, M., Irakulis-Loitxate, I., Gorroño, J., Guanter, L., Cusworth, D. H., and Aben, I.: Automated detection and monitoring of methane super-emitters using satellite data, *Gases/Machine Learning/Troposphere/Chemistry (chemical composition and reactions)*, <https://doi.org/10.5194/acp-2022-862>, 2023.

640 Sherwin, E. D., Rutherford, J. S., Chen, Y., Aminfar, S., Kort, E. A., Jackson, R. B., and Brandt, A. R.: Single-blind validation of space-based point-source detection and quantification of onshore methane emissions, *Sci Rep*, 13, 3836, <https://doi.org/10.1038/s41598-023-30761-2>, 2023.

What is the Methane Alert and Response System (MARS)? <https://unenvironment.widen.net/s/7pmjgcdgkz/mars-infographic-1>, last access: 1 August 2023.

Greenhouse Gas Equivalencies Calculator: <https://www.epa.gov/energy/greenhouse-gas-equivalencies-calculator#results>, last access: 22 September 2023.

645 Varon, D. J., Jacob, D. J., McKeever, J., Jervis, D., Durak, B. O. A., Xia, Y., and Huang, Y.: Quantifying methane point sources from fine-scale satellite observations of atmospheric methane plumes, *Atmospheric Measurement Techniques*, 11, 5673–5686, <https://doi.org/10.5194/amt-11-5673-2018>, 2018.

Gas Pipe Upgrades | Wales & West Utilities: <https://www.wwestutilities.co.uk/services/gas-pipe-upgrades/>, last access: 30 August 2023.

650 Webster, H. N., Whitehead, T., and Thomson, D. J.: Parameterizing Unresolved Mesoscale Motions in Atmospheric Dispersion Models, *Journal of Applied Meteorology and Climatology*, 57, 645–657, <https://doi.org/10.1175/JAMC-D-17-0075.1>, 2018.

Zazzeri, G., Lowry, D., Fisher, R. E., France, J. L., Lanoisellé, M., and Nisbet, E. G.: Plume mapping and isotopic characterisation of anthropogenic methane sources, *Atmospheric Environment*, 110, 151–162, <https://doi.org/10.1016/j.atmosenv.2015.03.029>, 2015.